The Magnitude of the Allosteric Conformational Transition of Aspartate Transcarbamylase Is Altered by Mutations†

Vince J. LiCata,* David S. Burz,‡ Nathan J. Moerke,§ and Norma M. Allewell

Department of Biochemistry, University of Minnesota, 1479 Gortner Avenue, St. Paul, Minnesota 55108

Received May 8, 1998; Revised Manuscript Received August 24, 1998

ABSTRACT: Global conformational transitions are of central functional importance for many enzymes and binding proteins. It is not known, however, how much variability can exist in such structural−functional linkages. We have characterized the global magnitude of the T to R conformational transition of *Escherichia coli* aspartate transcarbamylase (ATCase) by measuring (1) hydration changes using osmotic stress and (2) hydrodynamic changes using high-precision analytical gel chromatography. We find that specific mutations can alter the structural magnitude of the enzyme's conformational transition without abolishing allostery, suggesting that some degree of plasticity exists in the conformational component of allostery.

Aspartate transcarbamylase (ATCase)[1] from *Escherichia coli* exhibits all major types of functional molecular allostery: cooperative ligand binding, heterotropic allosteric regulation, negatively cooperative binding of identical allosteric effectors, functional synergy between different allosteric effectors, and a long-range Bohr effect (regulation by non-active site protonation). The enzyme catalyzes the first committed step in the biosynthesis of pyrimidines, the condensation of aspartate and carbamyl phosphate to form carbamyl aspartic acid. Aspartate binding is positively cooperative. The enzyme is a dodecamer comprised of six catalytic (33 kDa) and six regulatory (17 kDa) chains arranged as two catalytic trimers (c_3) and three regulatory dimers (r_2).

Regulation of cooperative substrate binding involves a dramatic quaternary structural shift from a low-affinity T-state conformation to a high-affinity R-state conformation. Crystal structures of the T and R conformations reveal major changes in the molecular architecture of the enzyme, including a 12 Å expansion along the 3-fold molecular axis, elimination of contacts between catalytic trimers, restructuring of several intersubunit interfaces, and closure of the aspartate and carbamyl phosphate binding domains in the catalytic chains (*8*−*15*) (see Figure 1). Detailed examination of the structures identifies many residues which are involved in the T to R switch, i.e., residues that undergo translational displacements, conformational alterations, or alterations in their pairwise interactions. Mutational studies likewise have identified numerous sites which alter the cooperativity of ligand binding. What is not known, in ATCase or any other allosteric system, is the level of structural precision required of the allosterically linked conformational change. In this study, we show that specific mutations can alter the global magnitude of the T to R transition of ATCase without abolishing cooperative ligand binding.

Hydration and Hydrodynamics

The osmotic stress technique uses the thermodynamic linkage between induced osmotic pressure (Π) and the equilibrium of a macromolecular process to evaluate the change in the molecular stoichiometry of the water associated with that process (*1*−*3*). When the osmotic pressure of the bulk solution is increased in a controlled manner by the addition of inert solutes, movement of water away from osmotically stressed (solute excluded) spaces on the macromolecule is favored. Macromolecular processes involving water uptake will be inhibited, while those involving water release to the bulk will be enhanced. We have recently shown that ATCase takes up ∼208 water molecules as it binds ligands and switches from the T to R conformation (*4*) and that excellent agreement exists between hydration changes measured by osmotic stress and those predicted by structure-based accessible surface area calculations (*4*, *16*). Here we examine hydration changes upon ligand binding for several mutants of ATCase that are altered at sites known to be involved in the T to R transition and use these changes as a gauge for relative global changes in the magnitude of the T to R transition.

Analytical gel chromatography (*5*, *6*) is a sensitive probe of molecular size and shape, and has been successfully used to detect and analyze the T to R conformational change of ATCase (*7*). The ligand binding-induced quaternary structure change of ATCase is readily detected as a change in

† Supported by NIH Grant DK-17335 (to N.M.A.) and the University of Minnesota.

* Please address correspondence to V. J. LiCata at his present address: The Department of Biological Sciences, Louisiana State University, Baton Rouge, LA 70803.

‡ Current address: Wadsworth Center, New York State Department of Health, Division of Genetic Disorders, Axelrod Institute, Albany, NY 12208.

§ Current address: Biological and Biomedical Sciences Program, Harvard Medical School, Boston, MA 02115.

[1] Abbreviations: ATCase, aspartate transcarbamylase; c_3, catalytic trimer; PALA, *N*-(phosphonoacetyl)-L-aspartic acid; PEG, polyethylene glycol; atm, atmospheres.

10.1021/bi981073m CCC: $15.00
Published on Web 11/20/1998

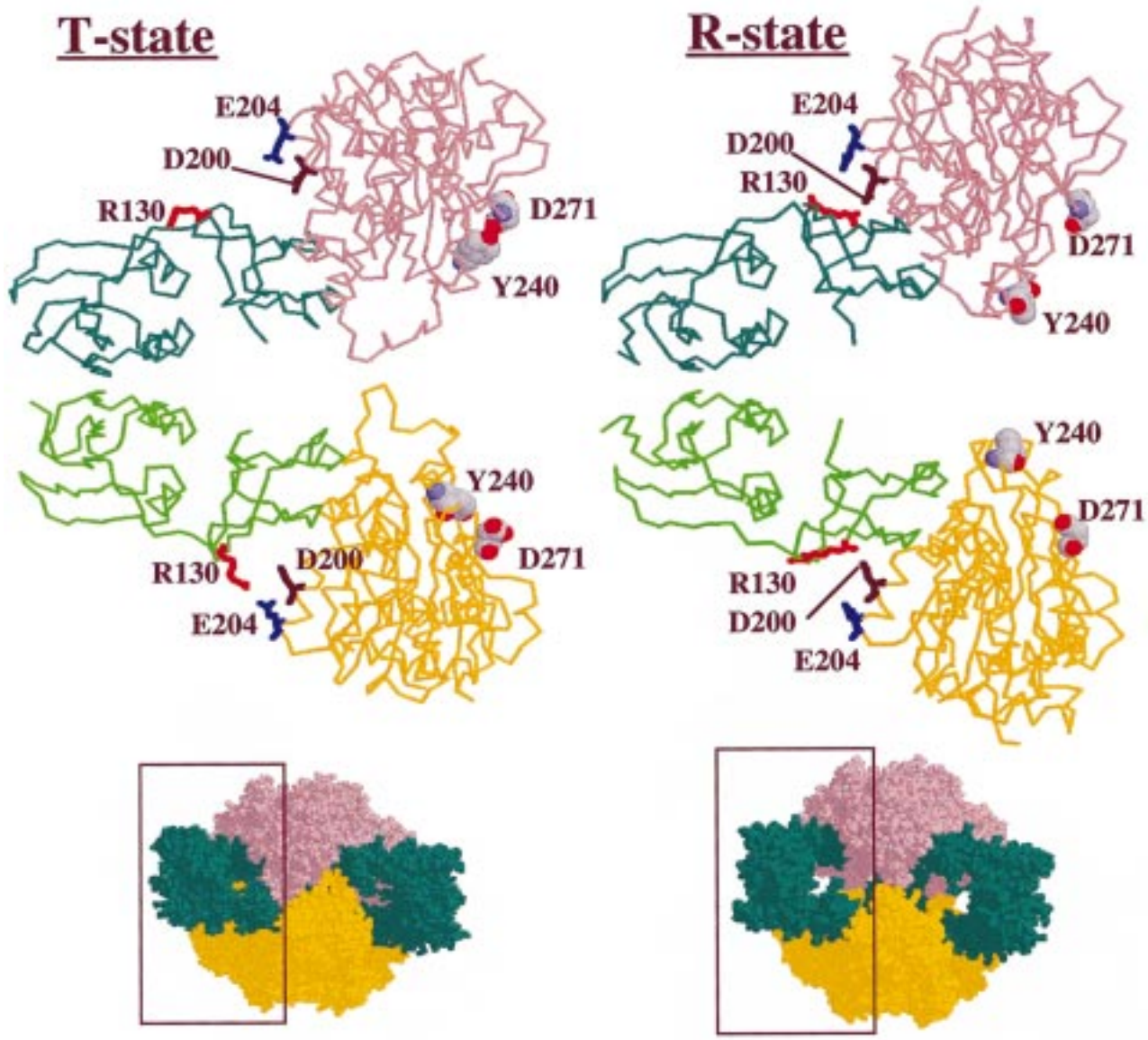

FIGURE 1: Structures of wild-type ATCase in the T and R conformations. Shown are PDB entries 6AT1 (unligated) (*13*) and 8ATC (PALA-ligated) (*10*−*12*). The upper portion of the figure shows the T- and R-state crystallographic asymmetric units with the locations of the mutated residues examined in this study. The lower portion shows the T- and R-state holoenzymes viewed along their molecular 2-fold axes. The boxes denote the approximate position of one asymmetric unit within the holoenzyme. In both the upper and lower sections, regulatory dimers are green, while the upper and lower catalytic trimers are pink and yellow, respectively. The space-filled residues show positions $Y240_c$ and $D271_c$. The red wire-frame residue is $R130_r$; $E204_c$ is blue, and $D200_c$ is black. Subscript letters c and r denote catalytic chain and regulatory chain sites, respectively.

elution volume, and hence partition coefficient (σ), during gel permeation chromatography of ATCase on carefully calibrated Sephacryl columns. Analytical gel chromatography and osmotic stress, two very different techniques, report the same hierarchy of structural size changes for the mutants examined.

It should also be noted that rather than measuring the difference between two discrete, singular T and R structures, it is possible that these techniques report the net difference between T and R conformational distributions (i.e., a family of T structures and a family of R structures). We mention this because the potential to detect differences between two different families of conformers has been suggested in previous osmotic stress studies (*17*), and in fact, an alternate wild-type ATCase R-state conformation has recently been observed by solution X-ray scattering (*18*). In this view, different mutations might either alter the population distribution within the T and/or the R family of conformers, or change the number of energetically accessible conformers in the T and/or R populations. In the absence of further evidence of the existence of such conformational distributions or conformer families, we interpret our current results in terms of two predominant and relatively discrete conformations.

Sites Examined

Figure 1 shows the locations of the mutations examined. Catalytic chain residues $Y240_c$ and $D271_c$ form an intrachain pairwise interaction within a cluster of interactions near the c1−c4 interface in the T state which is disrupted in the R state. Residue $Y240_c$ is tucked away from the trimer−trimer interface in the T state in its interaction with $D271_c$, but this

interaction is implicated in helping stabilize the T-state conformation. In the R state, $Y240_c$ points toward the opposite trimer, and in fact represents the closest approach between the two trimers in the R state (*8*−*15*).

Regulatory chain residue $R130_r$ exhibits two asymmetric conformations in the T-state structure. In half of the asymmetric unit, and thus half of the c−r interfaces, $R130_r$ forms a salt bridge with catalytic chain residue $E204_c$. In the other three T-state c−r interfaces, $R130_r$ points away from the interface. All T-state structures of ATCase exhibit this asymmetry for $R130_r$ (*8*−*15*). In the R state, $R130_r$ exhibits one conformation, forming a new salt bridge with catalytic chain residue $D200_c$ (*8*−*15*). The $R130_r$ salt bridge switch is "the single major conformational change that occurs in the entire c−r interface" during the T to R transition, and has been shown by mutagenesis to be required for normal cooperative function (*19*). No relationship, however, has been detected between the structural asymmetry of the T state and the function of the enzyme (*19*).

METHODS

ATCase and mutants were isolated from *E. coli* strain EK1104 transformed with the appropriate plasmid as described previously (*20*). EK1104 and plasmids containing the wild type and mutant genes were provided by E. R. Kantrowitz (Department of Chemistry, Boston College, Chestnut Hill, MA 02167). Solutes for osmotic stress experiments were purchased from Fluka Chemika-Biochemika (Milwaukee, WI), all other chemicals were from Sigma Chemical Co. (St. Louis, MO).

Enzymatic assays and osmotic stress measurements were performed in a buffer containing 20 mM Tris-HCl [tris(hydroxymethyl)aminomethane hydrochloride], 20 mM bis-Tris [bis(2-hydroxyethyl)iminotris(hydroxymethyl)methane], 20 mM CAPS [3-(cyclohexylamino)-1-propanesulfonic acid], 0.2 mM dithiothreitol, 0.2 mM EDTA (ethylenediaminetetraacetic acid), and a saturating amount of carbamyl phosphate (4.8 mM), at pH 8.3 and 25 °C, as described previously (*4*). ATCase holoenzyme kinetic data were fit using an equation which takes into account the substrate inhibition of the enzyme (*21*), and osmotic stress results were analyzed using thermodynamic relationships developed previously (*1*−*3*). Briefly, the change in the number of associated water molecules is obtained from the relationship

$$\frac{\partial kT \ln(K_m^{\Pi}/K_m^{0})}{\partial \Pi_{osm}} = \Delta V_w = \Delta N_w \times 30\ \text{Å}^3$$

where K_m^{Π} is the K_m at osmotic pressure Π, K_m^{0} is the K_m in the absence of added solute, ΔV_w is the linked change in volume, 30 Å^3 is the molecular volume of water, and ΔN_w is the linked change in the number of associated waters (*1*−*3*). To measure the total hydration change for a reaction, solutes which are excluded from all differentially hydrating spaces on the molecule(s) must be utilized (*3*, *16*). For the ATCase holoenzyme, stressing solutes with a MW of >3000 are required (*4*, *16*). Analytical gel chromatography was carried out in 40 mM potassium phosphate, 0.2 mM DTT, and 0.2 mM EDTA, at pH 7 and 5 °C, as described previously (*7*, *22*).

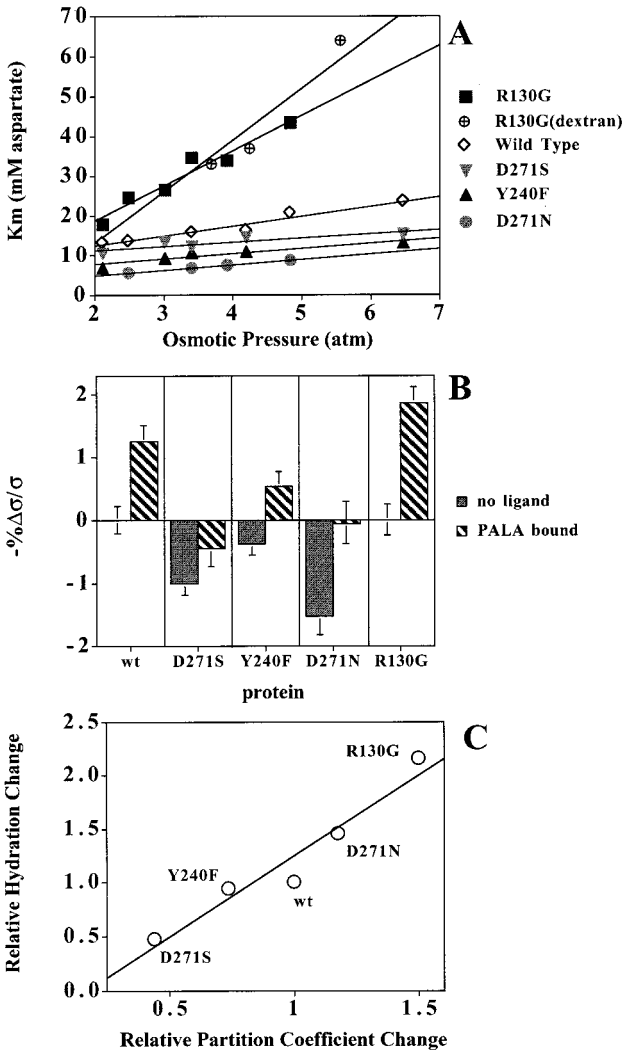

FIGURE 2: (A) Solute-induced osmotic pressure dependence of K_m for wild-type and mutant ATCases. Polyethylene glycol 8000 was used to raise the osmotic pressure. For mutant $R130G_r$, dextran 11000 was also used. Data for wild-type ATCase are from LiCata and Allewell (*4*). (B) Negative normalized relative percent changes in partition coefficients (σ) for wild-type and mutant ATCases in the presence and absence of the bisubstrate analogue PALA ($-\%\Delta\sigma/\sigma$). All measurements are normalized relative to wild-type ATCase in the absence of ligand. A decrease in the relative partition coefficient reflects an increase in the effective Stokes radius of the protein (*5*−*7*). Therefore, graphed as shown, increasing values indicate increasing relative Stokes radii or hydrodynamic sizes. (C) Correlation between the relative hydration changes associated with the T to R transition, determined by osmotic stress, and the normalized partition coefficient changes associated with the T to R transition, determined by gel chromatography, for the mutants examined in this study.

RESULTS AND DISCUSSION

Figure 2A shows the change in K_m at pH 8.3 for ATCase mutants $Y240F_c$, $D271N_c$, $D271S_c$, and $R130G_r$ as a function of increasing osmotic pressure. These dependencies yield the changes in water uptake linked to substrate binding (ΔH_2O, see Methods), and are reported in Table 1. The most dramatic and statistically significant hydration change relative to wild type is that observed for mutant $R130G_r$, which takes up approximately twice as much water as wild-type ATCase. A definite hierarchy exists for the other mutants relative to wild type. There is often scatter in osmotic stress data,

Table 1: Hydration Changes and Hill Coefficients for Wild-Type and Mutant ATCases

protein	ΔH_2O	Hill coefficient
wild type	189 ± 34	3.6 ± 0.6
Y240F	178 ± 97	2.1 ± 0.3
D271S	90 ± 71	2.7 ± 0.6
D271N	274 ± 22	4.4 ± 1.5
R130G	407 ± 117	2.4 ± 0.3
R130G (dextran)	493 ± 54	2.4 ± 0.3

presumably due to the difficulties of working with highly viscous solutions, and this is reflected in the associated errors reported in Table 1.

Solutes with a MW of >3000 report the total hydration change for the ATCase holoenzyme (*4*, *16*); hence, the osmotic pressures in Figure 2A were induced by PEG 8000 (polyethylene glycol with a molecular weight of 8000). Since $R130G_r$ exhibits the most dramatic shift in osmotic stress dependence relative to the wild type, results using dextran 11000 (MW) are also shown. The use of chemically different solutes is a powerful control against a number of potential artifacts in the application of osmotic stress (*1*−*4*, *16*). The hydration changes calculated for R130G using PEG 8000 versus dextran 11000 are within experimental error of one another; however, they may be indicative of an overlying solute specific effect. When the hydration change is calculated using osmotic stress, the observed volume change is generally assumed to be completely due to the movement of water, with no contributions from the solute, although it is understood that there can be solute contributions (*3*, *17*). This is an important issue in terms of understanding the theoretical and thermodynamic bases of osmotic stress effects. Timasheff has recently published that while it is theoretically incorrect to assume that the stressing solutes are entirely inert, "the experiments have produced correct numerical values of changes in preferential hydration" (*23*). The results of Figure 2A, along with our previous examination of wild-type ATCase using a variety of stressing solutes (*4*), indicate that for the holoenzyme any solute specific effects are relatively small, as all the fully excluded stressing solutes used generally report hydration changes that are within experimental error of one another.

Another control in ATCase is the assay of heterotropic allosteric activation by ATP and inhibition by CTP (*4*, *16*). The relative activity of $R130G_r$ at its K_m at an osmotic pressure of 4.8 atm in the presence of saturating ATP (∼208%) or CTP (∼72%) (Figure 3) is nearly identical to that in the absence of osmotic stress (*19*), indicating that the enzyme is not dissociated by osmotic stress, that its long-range heterotropic allosteric functions are intact, and that neither allosteric effector significanly alters the magnitude of the hydration change. This is essentially identical to the results observed with wild-type ATCase[24].

We have recently shown for wild-type ATCase that the accessible surface area change predicted by assuming each newly associating water covers 7−10 Å^2 of surface area (*1*) is nearly identical to the change in accessible surface area calculated directly from the T and R crystal structures (*4*). Similar agreement is found for the T to R transition of human hemoglobin (*1*, *16*). This strongly suggests that the hydration change determined by osmotic stress can be used to gauge

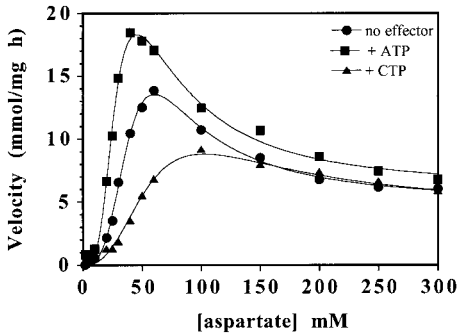

FIGURE 3: Heterotropic regulation of R130G ATCase by nucleotides at an osmotic pressure of 4.8 atm (induced with PEG 8000). Full aspartate titrations are shown in the absence of added nucleotides and in the presence of either 2 mM ATP or CTP.

the magnitude of the conformational change associated with the T to R transition of ATCase.

Results of analytical gel chromatography of wild-type ATCase and mutants $Y240F_c$, $D271N_c$, $D271S_c$, and $R130G_r$ in the presence and absence of the bisubstrate analogue PALA [*N*-(phosphonoacetyl)-L-aspartate] are shown in Figure 2B (*22*). Data are normalized relative to wild-type unligated ATCase. All the proteins show an increase in hydrodynamic size upon ligation and transition from the T to R conformation. The difference between the unligated and ligated relative partition coefficients reflects the relative change in the structural magnitude of the T to R transition for each mutant protein. Figure 2C shows that the size changes determined by gel chromatography correlate well with those determined by osmotic stress. Note that these experiments were conducted at pH 7 and 5 °C, in a buffer different from that used in the osmotic stress measurements, and using PALA to induce the conformational change. Despite this, the predicted hierarchy of T to R size changes is the same. The chromatographic behavior of wild-type ATCase was comparable in a variety of different buffers (data not shown) (*22*). The fact that the slope of the correlation of Figure 2C is greater than 1 may reflect a dependence of the magnitude of the conformational change on pH.

Results from both osmotic stress and gel chromatography show that the conformational transition of mutant $R130G_r$ deviates most from the wild type among the mutants examined. The results of Figure 2 clearly indicate that the salt bridge switch involving $R130_r$ (see Figure 1) is important in regulating the structural magnitude of the T to R conformational transition. The solvent accessible surface area of wild-type ATCase increases by ∼1600 Å^2 during the T to R transition (an increase of ∼1.6% in the total accessible surface area) (*4*). The hydration change for $R130G_r$ predicts the differential exposure of an additional ∼1900 Å^2 of surface area in the mutant and/or an increase in the volume change of the central cavity of the enzyme. Gel chromatography of $R130G_r$ reports that the increase in the magnitude of the T to R transition is due to an increase in the hydrodynamic size of the R state (Figure 2B). Further, the thermal stability of $R130G_r$ has been shown to be decreased slightly relative to that of the wild type; T_m shifts from 55 (wild type) to 49 °C ($R130G_r$), based on activity assays, and unlike the wild type, $R130G_r$ shows little or no cooperativity of thermal denaturation (*19*). Measuring denaturation by loss of activity primarily monitors

the R state of the enzyme; thus, these findings correspondingly suggest that the larger T to R transition we observe is primarily due to a more expanded, more loosely associated R state for $R130G_r$.

The behavior of $R130G_r$ is also relevant to understanding the molecular origins of metabolic disorders. In the absence of induced osmotic pressure, Figure 2A shows that the K_m for aspartate for $R130G_r$ is very similar to that of the wild type, such that it might not be targeted as being potentially significantly deleterious in vivo. As the osmotic pressure is raised toward the physiological osmotic pressure of ~7.6 atm (*25*), however, it becomes clear that mutant $R130G_r$ would have significant loss of activity in vivo.

At position 271_c, the difference between replacing D with N versus S can be most simply attributed to the greater chemical similarity between N and D and a better potential for $D271N_c$ to hydrogen bond to $Y240_c$. This simplest atomic interpretation for the behavior of the mutations at position 271_c focuses primarily on the T-state interaction of this residue. However, the fact that $Y240F_c$ behaves like the wild type although it can no longer hydrogen bond with position 271 suggests either that the $Y240_c-D271_c$ interaction has some hydrophobic character (e.g., interaction of the phenyl ring with the methylenes of $D271_c$) or that the R-state positions of these two residues are the more strongly linked to the global structural magnitude of the T to R transition. For example, the close approach of the $Y240_c$ side chains from opposite trimers in the R state may be the more critical role for $Y240_c$ in maintaining the structural precision of the T to R transition, and be relatively unaffected by the hydrophobically conservative Y240F substitution.

Hill coefficients for ATCase can differ substantially depending on experimental conditions (*21*, *26*). Table 1 shows that all mutants examined retain cooperativity under our assay conditions. There is no direct correlation between the apparent cooperativity and the relative magnitude of the T to R transition. Mutations that alter cooperativity have been identified and characterized in many allosteric systems, including ATCase. What this study shows, however, for the first time in any system, is that there can exist plasticity in the overlap between cooperative ligand binding and the magnitude of the associated conformational change for an allosteric system. As further structural details emerge for these and other mutants of ATCase, it will begin to be possible to clarify just which structural elements of the canonical T to R transition are crucial for allostery, and to understand which sites or regions of the protein are not so precisely structure−function coupled.

REFERENCES

1. Colombo, M. F., Rau, D. C., and Parsegian, V. A. (1992) *Science 256*, 655−659.
2. Rand, R. P., Fuller, N. L., Butko, P., Francis, G., and Nicholls, P. (1993) *Biochemistry 32*, 5925−5929.
3. Parsegian, V. A., Rand, R. P., and Rau, D. C. (1995) *Methods Enzymol. 259*, 43−94.
4. LiCata, V. J., and Allewell, N. M. (1997) *Biochemistry 36*, 10161−10167.
5. Ackers, G. K. (1970) *Adv. Protein Chem. 23*, 343−446.
6. Valdes, R., Jr., and Ackers, G. K. (1979) *Methods Enzymol. 61*, 125−142.
7. Bromberg, S., Burz, D. S., and Allewell, N. M. (1990) *J. Biochem. Biophys. Methods 20*, 143−156.
8. Honzatko, R. B., Crawford, J. L., Manaco, H. L., Ladner, J. E., Edwards, B. F. P., Evans, D. R., Warren, S. G., Wiley, D. C., Ladner, R. C., and Lipscomb, W. N. (1982) *J. Mol. Biol. 160*, 219−263.
9. Ke, H. M., Honzatko, R. B., and Lipscomb, W. N. (1984) *Proc. Natl. Acad. Sci. U.S.A. 81*, 4037−4040.
10. Ke, H., Lipscomb, W. N., Cho, Y., and Honzatko, R. B. (1988) *J. Mol. Biol. 204*, 725−747.
11. Krause, K. L., Volz, K. W., and Lipscomb, W. N. (1985) *Proc. Natl. Acad. Sci. U.S.A. 82*, 1643−1647.
12. Krause, K. L., Volz, K. W., and Lipscomb, W. N. (1987) *J. Mol. Biol. 193*, 527−553.
13. Stevens, R. C., Gouaux, J. E., and Lipscomb, W. N. (1990) *Biochemistry 29*, 7691−7701.
14. Lipscomb, W. N. (1992) *Proc. Robert A. Welch Found. Conf. Chem. Res. 36*, 103−143.
15. Lipscomb, W. N. (1994) *Adv. Enzymol. Relat. Areas Mol. Biol. 68*, 67−151.
16. LiCata, V. J., and Allewell, N. M. (1998) *Methods Enzymol. 295*, 42−62.
17. Reid, C., and Rand, R. P. (1997) *Biophys. J. 72*, 1022−1030.
18. Svergun, D. I., Barberato, C., Koch, M. H., Fetler, L., and Vachette, P. (1997) *Proteins 27*, 110−117.
19. Stebbins, J. W., and Kantrowitz, E. R. (1989) *J. Biol. Chem. 264*, 14860−14864.
20. Nowlan, S. F., and Kantrowitz, E. R. (1985) *J. Biol. Chem. 260*, 14712−14716.
21. LiCata, V. J., and Allewell, N. M. (1997) *Biophys. Chem. 64*, 225−234.
22. Burz, D. S. (1990) Ph.D. Dissertation, Wesleyan University, Middletown, CT.
23. Timasheff, S. N. (1998) *Proc. Natl. Acad. Sci. U.S.A. 95*, 7363−7367.
24. LiCata, V. J., and Allewell, N. M. (1998) *Biochim. Biophys. Acta 1384*, 306−314.
25. Stock, J. B., Rauch, B., and Roseman, S. (1977) *J. Biol. Chem. 252*, 7850−7861.
26. Allewell, N. M., and LiCata, V. J. (1995) *Methods Enzymol. 259*, 608−628.

BI981073M